Effect of cable sheath termination on transient overvoltages due to high-frequency cable-transformer resonance

Behdani, Behzad; Niasar, Mohamad Ghaffarian; Popov, Marjan

Important note
To cite this publication, please use the final published version (if applicable).
Please check the document version above.

Effect of cable sheath termination on transient overvoltages due to high-frequency cable-transformer resonance☆,☆☆

Behzad Behdani, Mohamad Ghaffarian Niasar, Marjan Popov *

Delft University of Technology, Faculty of EEMCS, Mekelweg 4, 2628 CD Delft, The Netherlands

ARTICLE INFO

ABSTRACT

High-frequency resonances in cable-transformer systems can result in excessive overvoltages, increasing the probability of insulation failure for critical components such as power transformers. These resonances occur due to the interaction between the cable and transformer and are influenced by the cable's characteristics, including the length and wave propagation velocity. In addition, the terminating impedances of the cable's core and sheath conductors affect the resonance characteristic of the cable as well. Applying single-point sheath grounding to the high-voltage cable connecting the switchgear to the power transformer is conventional. This paper demonstrates that the cable-transformer resonances and resulting overvoltages can vary significantly depending on the end at which the sheath conductors are grounded. An in-depth investigation of such effects is carried out through rigorous mathematical analysis, followed by experimental validation and simulations in an electromagnetic transient (EMT)-based software using models that properly represent the equipment behaviors in a wide-frequency range. The results indicate that sheath conductor grounding configuration can profoundly affect the system response, influencing the severity of transient overvoltages caused by cable-transformer resonances.

1. Introduction

Transient overvoltages (OVs) emerge in power system components from internal origins, such as faults and circuit breaker (CB) switching operations, and external origins from lightning discharges. Modern power systems have become increasingly susceptible to transient OVs due to two factors. First, by the growing expansion and interconnection of the electrical network to meet the increasing energy demands, they have become more exposed to incidents such as faults and lightning strikes. Moreover, as the integration of renewable energy sources increases, the stochastic nature of these sources will lead to more frequent switching operations [1]. The resultant OVs stress the insulation material and shorten the lifetime of crucial components such as power transformers [2].

During transient events, electromagnetic energy is redistributed among system components. This process does not occur instantly, but in an oscillatory way following the system's natural resonance frequencies [3]. The resonance phenomenon is an inherent property of electrical circuits, where energy is periodically exchanged between

the circuit's capacitances and inductances. Consequently, mutual interactions in cable transformer systems introduce high-frequency (HF) resonances to the system, accompanied by OVs [4]. With the increasing application of cable-based power transmission and distribution in modern power systems, power transformers become more vulnerable to these undesirable effects.

Cable-transformer transient resonances attract considerable attention. The research work in [5] deals with resonances between the transformer and supplying cable, where severe OVs occurred on the transformer's secondary side during energization. Through detailed experimental and theoretical investigation, the study in [6] analyzed the contribution of the supplying cable to the amplification of transient surges distributed along transformer windings and internal resonant overvoltages during transformer energization by a vacuum circuit breaker (VCB). In [7], a transformer with accessible internal nodes was used to analyze the distribution of transient voltages along the windings for various supply cable lengths and secondary side terminations. HF cable-transformer resonances were studied in [8], highlighting several

topologies prone to resonances, such as ground faults and switching operations. In [9], a detailed analysis was carried out on cable-transformer resonances generated by VCB prestrike transients. A theoretical study conducted in [10] demonstrated that quarter-wavelength standing waves formed in the cable were the reason for mutual cable-transformer resonances, which led to excessive OVs at the transformer low-voltage (LV) side.

In high voltage (HV) cables, sheath conductors are usually grounded to provide a fault current return path, confine the electric fields within the insulation, and clamp the capacitive sheath voltage build-up during normal operation and transient phenomena [11]. While sheath conductors in long HV cables are often properly connected to the ground with solid- and cross-bonding arrangements, short cables connecting the switchgear to the power transformer are usually provided with a single-point sheath grounding. When the sheath is grounded at both ends, circulating currents are formed under normal operating conditions, leading to sheath losses and limitation of the cable's ampacity. By employing single-point sheath grounding, these circulating currents are eliminated, preventing such losses and ampacity limitations [12]. Other analyses performed on wave propagation and transient behavior of cable systems solely consider the response of coaxial modes, while the effect of sheath modes on cable's resonance frequencies is addressed in only a few studies [13–15]. Nevertheless, these studies have only focused on cross-bonded cables, neglecting the effect of single-point grounding arrangements.

This paper addresses the effect of sheath conductor termination on the transient response of HV cables. Initially, the sheath conductor termination effect on the cable's impedance response is assessed by using distributed-parameter cable equations. Subsequently, simulations are performed on a test system in EMTP to study the sheath conductor termination effect on cable-transformer resonances. To this end, proper models are applied to represent the behavior of system components in a wide frequency range; namely cables, power transformers, and grounding grids. Eventually, an experimental analysis is carried out to verify the effect of the end at which the metallic sheath is grounded on cable-transformer resonances. The results indicate that the end at which the sheath conductor is grounded significantly impacts cable-transformer resonances and, hence, the severity of prevailed transient OVs. It is shown that applying a single-point grounding of the cable's sheath at the transformer side results in the suppression of resonant OVs.

It is worth mentioning that the objective of this study is not to predict the OVs affecting specific installations in a particular power system but rather to demonstrate the effect of cable sheath terminations on the mutual cable-transformer resonant interactions in a general context. As it is supported by the theoretical analysis, the results of this study are not limited to the examined simulation and experimental setups but can be generally extended to any typical cable-transformer system.

The article is organized as follows. The sheath termination effect on cable resonances is analyzed in Section 2. The implemented test system is described in Section 3. In Section 4, resonances occurring between the cable and transformer are investigated considering different cable sheath terminations through EMTP simulations. In Section 5, the analysis is validated by measurements using an experimental test setup. The presented analysis is concluded in Section 6.

2. Theoretical analysis of cable resonances

An *n*-conductor cable system can be represented by the nodal admittance matrix $\mathbf{Y}_n$ in the frequency domain as [16]:

$$\begin{bmatrix} \mathbf{I}_s \\ \mathbf{I}_r \end{bmatrix} = \begin{bmatrix} \mathbf{Y}_e & \mathbf{Y}_m \\ \mathbf{Y}_m & \mathbf{Y}_e \end{bmatrix} \times \begin{bmatrix} \mathbf{V}_s \\ \mathbf{V}_r \end{bmatrix} \tag{1}$$
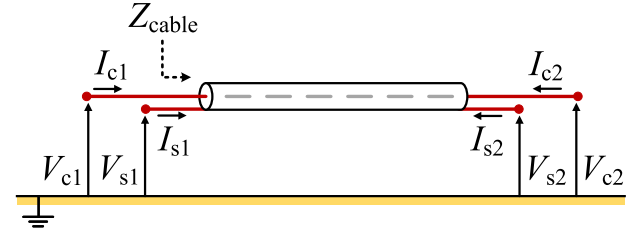

Fig. 1. Finite-length distributed-parameter cable section.

where **I** and **V** are $n \times 1$ current and voltage vectors at the sending- and receiving end, indicated by subscripts "s" and "r", respectively. The $n \times n$ matrices $\mathbf{Y}_e$ and $\mathbf{Y}_m$ are given by:

$$\mathbf{Y}_e = \mathbf{Y}_0 \coth(\mathbf{\Gamma} l) \tag{2}$$

$$\mathbf{Y}_m = -\mathbf{Y}_0 \operatorname{csch}(\mathbf{\Gamma} l) \tag{3}$$

where $\mathbf{Y}_0$ and $\mathbf{\Gamma}$ denote the characteristic admittance and propagation function matrices, and l is the line/cable length.

For the analysis, the cable section shown in Fig. 1 is considered. The relation between currents and voltages in the cable section is expressed by rewriting Eq. (1) in the following form:

$$\begin{bmatrix} I_{c1} \\ I_{s1} \\ \hline I_{c2} \\ I_{s2} \end{bmatrix} = \left[\begin{array}{cc|cc} A_{11} & A_{12} & B_{11} & B_{12} \\ A_{21} & A_{22} & B_{21} & B_{22} \\ \hline B_{11} & B_{12} & A_{11} & A_{12} \\ B_{21} & B_{22} & A_{21} & A_{22} \end{array} \right] \times \begin{bmatrix} V_{c1} \\ V_{s1} \\ \hline V_{c2} \\ V_{s2} \end{bmatrix} \tag{4}$$

where the elements of the nodal admittance matrix in (4) can be calculated according to the Appendix as:

$$\begin{aligned} A_{ij} &= a_{ij} \coth(\gamma l) \\ B_{ij} &= -b_{ij} \operatorname{csch}(\gamma l) \qquad ; i, j = 1, \dots, n \end{aligned} \tag{5}$$

As it is expressed in (5), all elements of the nodal admittance matrix $\mathbf{Y}_n$, including those corresponding to the core and sheath, have the same propagation function γ. The propagation function γ is a complex number in the form of $\gamma = \alpha + j\beta$, where α is the attenuation- and β is the phase coefficient, expressed in terms of the excitation frequency f and wave propagation velocity v' by $\beta = 2\pi f / v'$ [16]. Now, as it was shown that all conductors are characterized by the same propagation function γ, they will have the same phase coefficient β, and thus, it can be concluded that the wave propagates with the same velocity $v' = 2\pi f / \beta$ in all the conductors.

Resonance in electrical circuits occurs when electric and magnetic energies are balanced, that is, when the capacitive and inductive effects cancel each other [3]. This means that resonance conditions solely depend on the reactive elements of the circuit. In this regard, it is important to note that considering or disregarding the losses does not influence the conditions for resonance occurrence or the frequencies at which the resonance occurs. The resonance behavior of the cable under different sheath grounding configurations is analyzed by evaluating its short circuit (SC) impedance $Z_{\text{cable,SC}}$ for each case, as explained further in the text.

2.1. Solid grounding at both ends

Assuming that the sheath conductor is solidly grounded at both ends, $Z_{\text{cable,SC}}$ can be obtained by yielding $V_{c2} = V_{s1} = V_{s2} = 0$, as:

$$Z_{\text{cable,SC}} = \frac{1}{A_{11}} = a_{11}^{-1} \tanh(\gamma l) \tag{6}$$

For frequencies, $f_k = kv'/4l$, with k as an integer number, the phase coefficient becomes $\beta = jk\pi/2l$, and since $\gamma = \alpha + j\beta$, cable's impedance becomes purely resistive, as:

$$Z_{\text{cable,SC}}(f_k) = a_{11}^{-1} \tanh\left(\alpha l + jk\frac{\pi}{2}\right)$$

$$= \begin{cases} a_{11}^{-1} \coth(\alpha l) & \text{for odd } (k) \\ a_{11}^{-1} \tanh(\alpha l) & \text{for even } (k) \end{cases} \tag{7}$$

The coefficient α represents the cable losses, including the conductor and dielectric losses. According to (7), $Z_{\text{cable,SC}}$ varies between minima (for even values of k) and maxima (for odd values of k) over the frequency spectrum. This can be better understood assuming lossless cable where ($\alpha \to 0$). For this condition, $Z_{\text{cable,SC}}$ is obtained as:

$$\lim_{\alpha \to 0} Z_{\text{cable,SC}}(f_k) = \begin{cases} \infty & \text{for odd } (k) \\ 0 & \text{for even } (k) \end{cases} \tag{8}$$

As outlined above, frequencies f_k denote the cable's natural frequencies. For these frequencies, the cable length matches an integer multiple of a quarter (for odd k) or half (for even k) of the wavelength λ, expressed as $l = k\lambda/4$. As mentioned earlier, mutual cable-transformer resonances are created due to quarter-wavelength standing waves formed in the cable [10]. According to Eq. (8), these quarter-wavelength resonances are characterized by $Z_{\text{cable,SC}} \to \infty$. In order to determine whether the cable exhibits quarter-wave resonances under single-point sheath grounding configurations, in the following cases, it is evaluated whether $Z_{\text{cable,SC}}$ tends to infinity at the corresponding frequencies.

2.2. Single-point grounding at receiving end

Considering that the sheath conductor of the cable section in Fig. 1 is grounded only at the receiving end, $Z_{\text{cable,SC}}$ can be calculated by holding $V_{c2} = V_{s2} = 0$, while $V_{s1} \neq 0$ and $I_{s1} = 0$ in (4), as:

$$Z_{\text{cable,SC}} = \frac{A_{22}}{A_{11}A_{22} - A_{12}A_{21}}$$

$$= \frac{a_{22}}{a_{11}a_{22} - a_{12}a_{21}} \tanh(\gamma l) \tag{9}$$

Similar to above, neglecting losses ($\alpha \to 0$) for tractability, $Z_{\text{cable,SC}}$ can be obtained at resonance frequencies f_k as:

$$Z_{\text{cable,SC}}(f_k)\Big|_{\alpha \to 0} = \frac{a_{22}}{a_{11}a_{22} - a_{12}a_{21}} \tanh\left(jk\frac{\pi}{2}\right)$$

$$= \begin{cases} \infty & \text{for odd } (k) \\ 0 & \text{for even } (k) \end{cases} \tag{10}$$

As it can be seen from (10), since $Z_{\text{cable,SC}}$ tends to infinity at resonance frequencies f_k corresponding to odd values of k, it is concluded that the quarter-wavelength resonances are present in the cable response for single-point sheath grounding at the receiving end.

2.3. Single-point grounding at sending end

The effect of single-point sheath grounding at the sending end can be analyzed by applying these constraints $V_{c2} = V_{s1} = 0$, while $V_{s2} \neq 0$ and $I_{s2} = 0$ in (4), as:

$$Z_{\text{cable,SC}} = \frac{A_{22}}{A_{11}A_{22} - B_{12}B_{21}}$$

$$= \frac{a_{22} \sinh(2\gamma l)}{2a_{11}a_{22}\cosh^2(\gamma l) - 2b_{12}b_{21}} \tag{11}$$

Following the same approach as before, by considering a lossless cable ($\alpha \to 0$) to preserve tractability, $Z_{\text{cable,SC}}$ at resonance frequencies f_k is calculated as:

$$Z_{\text{cable,SC}}(f_k)\Big|_{\alpha \to 0} = \frac{\frac{1}{2}a_{22}\sinh(jk\pi)}{a_{11}a_{22}\cosh^2\left(jk\frac{\pi}{2}\right) - b_{12}b_{21}} = 0 \tag{12}$$
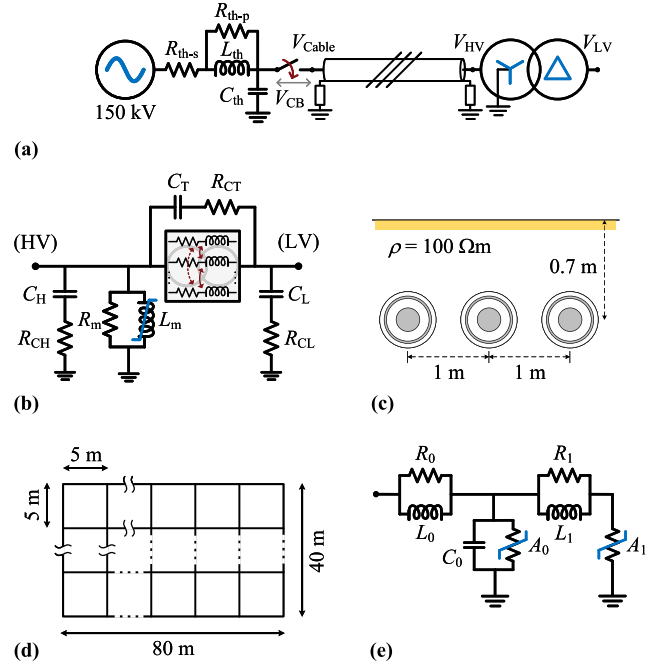

Fig. 2. The implemented test system: (a) network schematic, (b) power transformer, (c) cable, (d) grounding grid, (e) surge arrester.

According to Eq. (12), the value of $\sinh(jk\pi)$ is equal to zero for all integer multiples of k. Therefore, it is shown that the quarter-wavelength resonances are suppressed in the case of single-point sheath grounding at the sending end.

Next, the cable response under different sheath grounding configurations is studied through simulations.

3. Implemented simulation setup

To investigate the sheath conductor termination effect on cable-transformer resonances, a test setup, as shown in Fig. 2a, is simulated in EMTP. The system is supplied by a 150 kV grid with Thevenin equivalent parameters of $L_{\text{th}} = 100\,\text{mH}$, $R_{\text{th-s}} = 4\,\Omega$, $R_{\text{th-p}} = 398\,\Omega$, and $C_{\text{th}} = 2\,\mu\text{F}$. This section presents the components of the adopted test system in detail.

3.1. Power transformer

The power transformer model is shown in Fig. 2b. The simulations are carried out by applying the well-known BCTRAN model in EMTP [17]. From Fig. 2b, one can see that additional branches are added to account for the stray capacitances and the core's magnetization effects. Although the implemented BCTRAN model does not precisely replicate the transformer's wideband response, it sufficiently represents typical transformer behavior over a wide frequency band. Since this study does not aim to predict actual OVs, the implemented BCTRAN-based transformer model's typical response is adequate for analyzing the impact of cable sheath termination on cable-transformer interactions. Transformer parameters are shown in Table 1.

3.2. Cable

The cable is represented by a wideband universal line model [18]. Cable length is 78 m, and its cross-section is depicted in Fig. 2c. The specifications of the model are given in Table 2.

Table 1
Transformer model parameters.

Parameter	Unit	Value			
Transfer ratio	(kV)	150/11.2			
Nominal power	(MVA)	48			
Capacitances	(nF)	C_H	C_T	C_L	
		1.186	1.263	3.286	
Resistances	(Ω)	R_{CH}	R_{CT}	R_{CL}	R_m
		25	30	30	2.2×10^6
Inductance L_m	(A)	0.26	6.53	26.1	261
	(Wb)	325	374	400	503

Table 2
Short cable parameters.

Layer	Parameter and value		
Core conductor	$r = 21.8$ mm	$\rho = 2.65 \times 10^{-8}$ Ωm	$\mu_r = 1$
Core insulator	$r = 43$ mm	$\epsilon_r = 2.9$	$\mu_r = 1.163$
Sheath conductor	$r = 45.35$ mm	$\rho = 2.1 \times 10^{-7}$ Ωm	$\mu_r = 1$
Sheath insulator	$r = 50.5$ mm	$\epsilon_r = 2.3$	$\mu_r = 1.163$

r: radius, ρ: resistivity, ϵ_r: relative permittivity, μ_r: relative permeability.

According to [11], the resonance frequencies of the cable also depend on the cable length:

$$f_{\frac{k}{4}} = k \frac{1}{4\tau} = k \frac{v'}{4l} \tag{13}$$

where l is the cable length, τ the wave travel time, v' the propagation velocity, and k is an integer. However, as shown in Section 2, resonance suppression under single-point sheath grounding at transformer side is independent of the cable length.

3.3. Grounding grid

The grounding grid, as shown in Fig. 2d, consists of a meshed structure of bare conductors with no vertical rods, buried at a depth of 1 m. The soil is considered as a single-layer with a resistivity of 100 Ωm and relative permeability of 10. Three current draining terminals connect the grounding grid to the system above ground at points G_1 (20, 30) connected to transformer neutral, G_2 (40, 20) connected to SA drain, and G_3 (50, 20) connecting to cable sheath at the receiving end. The grounding of the cable's sending end sheath is considered ideal. TragSys software [19] is applied to calculate the grounding system response. This tool takes the geometrical data of the grounding grid, as well as the characteristics of the soil, such as resistivity and permeability, and solves the electromagnetic equations of the structure [20]. Using TragSys, impedances seen at the grounding terminals are obtained in the frequency domain and then implemented in EMTP by applying the vector fitting method [21,22]. Fig. 3 demonstrates the grounding grid impedances, including the self impedances seen from ground terminals and mutual impedances between ground terminals.

3.4. Surge arresters

Three types of surge arresters (SAs) are applied for the simulated test system: one for the sheath voltage limiter (SVL) of the cable and the others for transformer OV protection installed at the HV and LV side. The IEEE model of SA [23] is adopted, as shown in Fig. 2e. Table 3 presents the specifications of the implemented SAs.

3.5. Circuit breaker

The CB is modeled as shown in Fig. 4, consisting of a controlled ideal switch S placed in parallel to an RLC branch that represents the parasitic parameters of the gap between CB contacts. According to the flowchart in Fig. 4, prestriking transients are modeled by controlling
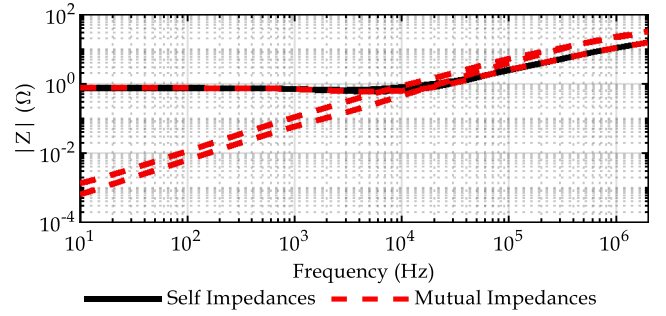

Fig. 3. Self- and mutual impedances observed from grounding grid terminals connected to the system.
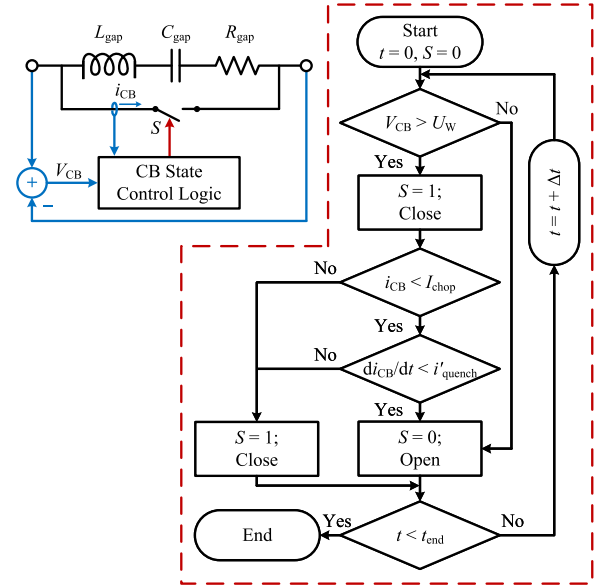

Fig. 4. The implemented model for CB.

the state of the switch S based on the contact gap withstand voltage U_W, the chopping current I_{chop}, and the high-frequency current quenching capability i'_{quench}, according to the following relationships [9]:

$$U_W = A(t - t_0) + B \tag{14}$$

$$i'_{quench} = C(t - t_0) + D \tag{15}$$

where t_0 is the contact closing time. The CB model parameters are adopted from [9], given by $I_{chop} = 3$ A, $A = -0.02$ kV/μs, $B = 0$ kV, $C = 0$ A/s^2, and $D = 350$ A/μs. Gap stray parameters R_{gap}, L_{gap}, and C_{gap} are equal to 100 Ω, 0.05 μH, and 0.1 nF, respectively.

4. Simulation results and discussion

This section presents the results from the simulation of the studied test system and discusses the effects of sheath conductor terminations on cable-transformer resonances.

4.1. Frequency-domain analysis

To better understand the effect of the sheath conductor's grounding configuration on cable-transformer resonant behavior, the system's response is assessed in the frequency domain. It is acknowledged

Table 3
Adopted surge arrester parameters.

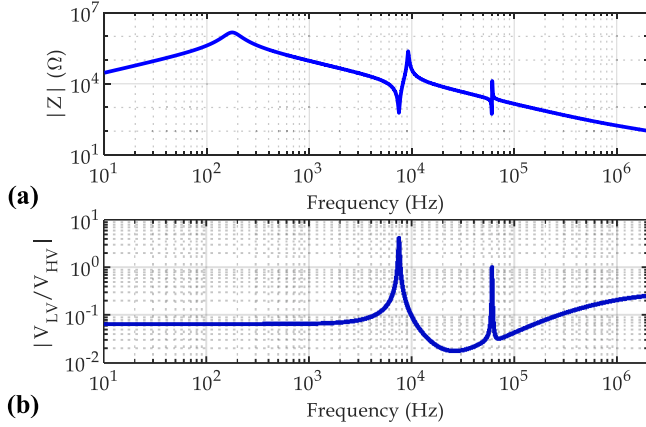| SA	Rated voltage (kV)	MCOV (kV)	Impulse current residual voltage (kV)		Height (cm)	No. columns
			30/60 μs 0.5 or 2 kA[a]	8/20 μs 10 kA		
HV	170	131	334	378	143	1
LV	15	13.3	31	40.8	20	1
SVL	7.2	6.5	15	18.8	21.1	1

[a] 0.5 kA for SVL and 2 kA for other SAs.

Fig. 5. Power transformer frequency response: (a) HV-side terminal impedance, (b) voltage transformation ratio.
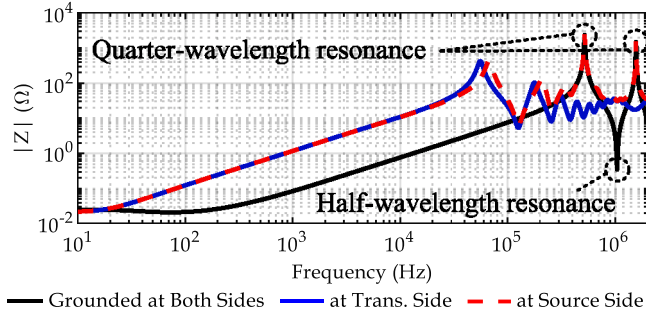

Fig. 6. Effect of different sheath grounding places on cable's impedance.

Fig. 7. Cable-transformer frequency response: (a) harmonic impedance, (b) voltage transformation ratio.

that cable-transformer resonant interactions are attributed to the cable's quarter-wavelength resonances occurring at the transformer terminal [10]. The HV-side terminal impedance of the transformer and its voltage transformation ratio are shown in Fig. 5a and b, respectively. As it can be seen in Fig. 5, the implemented BCTRAN-based transformer model reproduces the typical transformed behavior over a wide frequency range, satisfying the objective of this analysis.

The cable's impedance at the transformer's terminal is almost equal to its short-circuit impedance. The effect of different sheath grounding configurations on the cable's harmonic impedance is shown in Fig. 6. Fig. 6 confirms the theoretical analysis in Section 2, showing that the cable quarter-wave resonances are present for configurations with solid sheath grounding at both sides and single-point sheath grounding at the source side, whereas these resonances are absent when the sheath is only grounded at the transformer side. It is noteworthy that the first quarter-wave resonance of the cable is observed to occur at $f_{\frac{1}{4}} = 521$ kHz.

Consequently, the effect of different sheath grounding configurations on the mutual cable-transformer resonances can be analyzed through frequency domain responses shown in Fig. 7. One can see that the cable-transformer system resonance frequencies resulted in
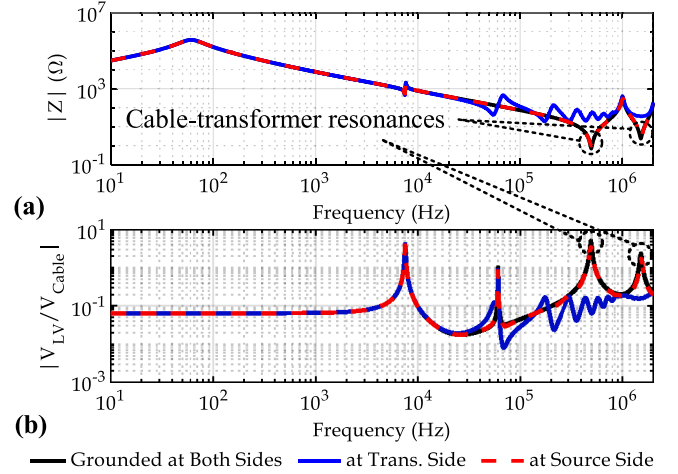
increased voltage amplifications. The dominant resonance frequency is 495 kHz. Similarly, the cable-transformer resonances are only present for configurations of solid sheath grounding provided at both sides and single-point sheath grounding provided at the source side. On the other hand, since cable quarter-wave resonances are suppressed when the sheath conductor is only grounded at the transformer side, no mutual cable-transformer resonances and resultant OVs occur for this configuration.

4.2. Time-domain analysis

To evaluate the effect of the cable's sheath grounding configuration on the system's behavior in the time domain, transient simulations under various conditions are performed in EMTP. To this aim, the cable-transformer system shown in Fig. 2a is energized by closing a circuit breaker (CB). The CB is represented according to [9], where the prestriking effect is also considered. The time-domain analysis is performed through the following cases.

4.2.1. Traveling wave response of cable

Initially, the time-domain response of the cable is analyzed by applying a step voltage at the sending end of each core and sheath conductor once at a time while all other terminals are short-circuited. The resultant propagating current waves at the sending and receiving ends of the corresponding under-test conductor are measured and demonstrated in Fig. 8. As it can be seen, the wave propagation speed in the core and sheath are equal, confirming the theoretical analyses in Section 2.

As indicated in Fig. 8, wave traveling time along the cable is equal to $\tau = 0.48$ μs. This is in line with the first quarter-wave resonance frequency $f_{\frac{1}{4}} = 521$ kHz, according to (13).
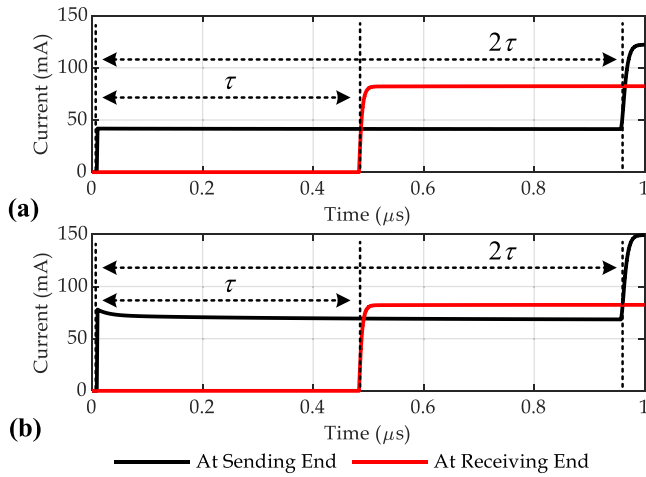
Fig. 8. Traveling wave response of the cable system: (a) core conductor, (b) sheath conductor.
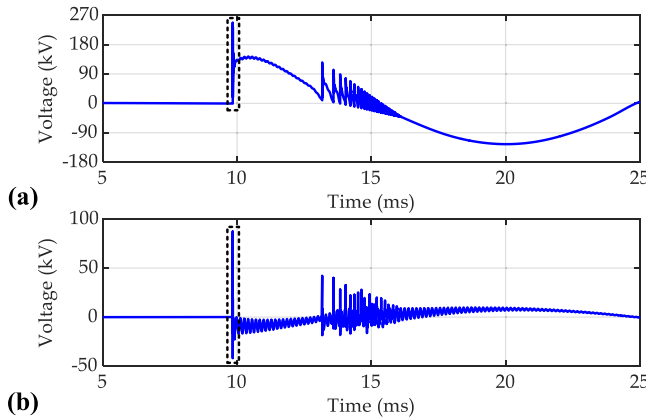

Fig. 9. Cable-transformer system energization transients: (a) transformer HV side voltage, (b) transformer LV side voltage.

4.2.2. Cable-transformer energization transients

The energization transients are simulated for the adopted test system in Fig. 2 by closing the CB. As a result, OVs are generated on transformer HV and LV terminals, as shown in Fig. 9. Initially, no surge protective devices (SPDs) are employed in the test system. It is worth mentioning that the CB closing time is chosen in a way the first striking surge occurs around the maximum amplitude of the supply voltage. From Fig. 9, it can be seen that multiple prestrikes occur as the CB contacts close; however, for clarity, the focus is put on the first prestrike.

The effects of the two single-point sheath grounding configurations at the source and transformer sides have been compared with the solid sheath grounding at both sides during the first energization prestriking transient in Figs. 10 and 11, respectively. The duration of the cable-transformer resonance oscillations, as marked in Fig. 10, is equal to 2.02 μs, which corresponds to the cable-transformer resonance frequency of 495 kHz observed in the previous sub-section. It is evident in Fig. 10 that the mutual cable-transformer resonances occur for the two configurations of solid sheath grounding at both sides and single-point sheath grounding at the source side, leading to severe OVs at transformer terminals. In contrast, Fig. 11 shows that such resonances are suppressed when the sheath is only grounded at the transformer side. Accordingly, the magnitudes of the OVs imposed on the transformer are much lower as well.
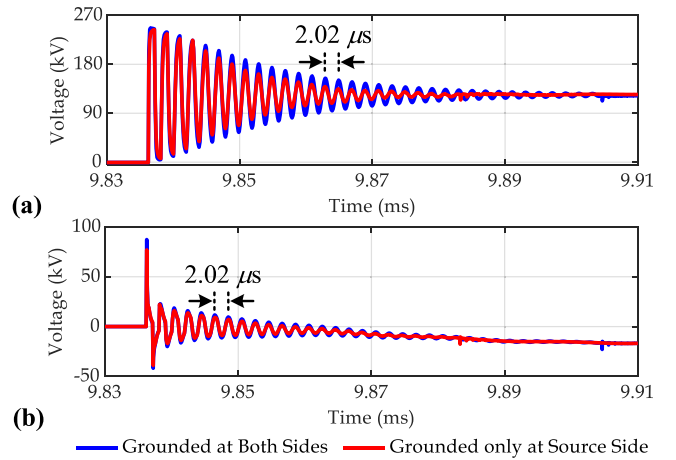

Fig. 10. Effect of single-point sheath grounding at source side in comparison with solid sheath grounding at both sides during the first energization prestrike: (a) transformer HV side voltage, (b) transformer LV side voltage.
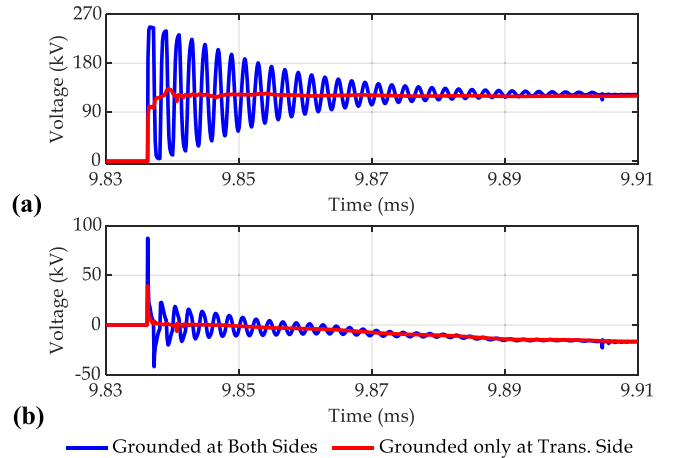

Fig. 11. Effect of single-point sheath grounding at transformer side in comparison with solid sheath grounding at both sides during first energization prestrike: (a) transformer HV side voltage, (b) transformer LV side voltage.

4.2.3. Effect of SPDs

As it was shown, when the cable's sheath is only grounded at the transformer side, the resonances are suppressed, and OVs are mitigated. However, as shown in 12a, the open-circuit (OC) end of the sheath (at the source side) can be exposed to severe OV surges, causing cable jacket insulation breakdown. Therefore, an SVL, in the form of an SA as introduced in Section 3, is applied to the sheath conductor at the source side, which is the opposite side of the grounded end. The resultant sheath voltage in the presence of the SVL is shown in Fig. 12b.

Because the SVL is installed at the source side, the cable's sheath grounding configuration depends on the SVL's operating condition. Specifically, when the SVL is not conducting current, the sheath will have a single grounding point at the transformer side. Conversely, when the SVL is conducting, the sheath can be considered grounded at both ends. Accordingly, the mutual cable-transformer resonances and their resulting OVs will also depend on the operating status of the SVL. The transformer terminal voltages with- and without applying SVL to the caple's sheath at the source side are shown in Fig. 13. As can be seen, at the instant of the prestriking surge, when the SVL is activated, the sheath conductor will behave as grounded on both sides, and several oscillations of resonating OVs will occur at the transformer's terminals. Nevertheless, as soon as the SVL is deactivated, the cable-transformer resonances are suppressed.
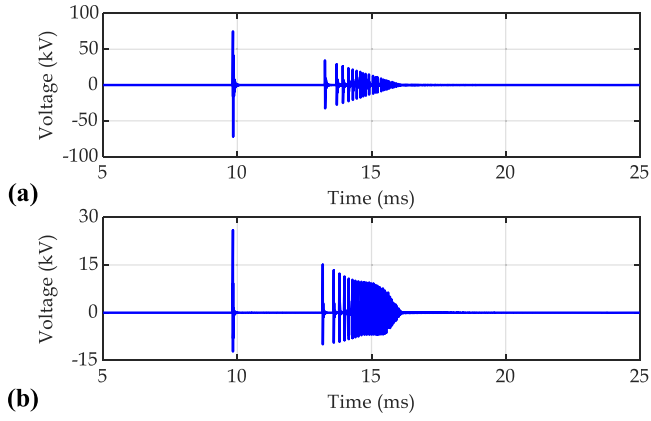
(a)

(b)

Fig. 12. Sheath voltage at source side while sheath is grounded at transformer side: (a) sheath at source side open, (b) SVL applied at the source side.

(a)

(b)

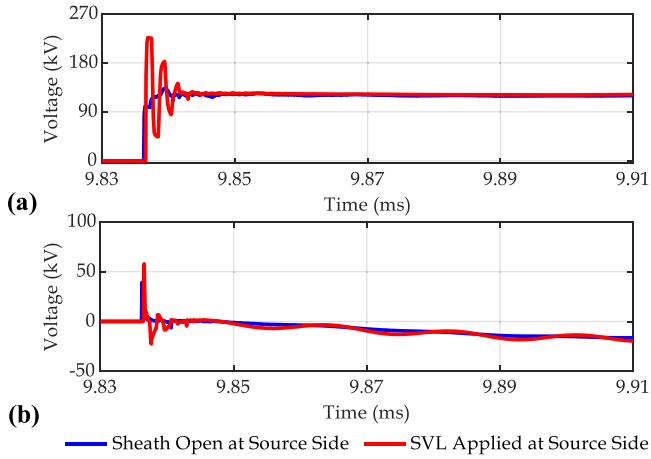— Sheath Open at Source Side — SVL Applied at Source Side

Fig. 13. Effect of SVL on cable-transformer system energization transients under single-point sheath grounding configuration at transformer side: (a) transformer HV side voltage, (b) transformer LV side voltage.

Ultimately, SAs are applied, as introduced in Section 3, to provide OV protection for the transformer. The effect of SPDs on the transformer terminal voltages during the first energization prestriking transients is shown in Fig. 14. Although it was shown earlier that resonating OVs are suppressed when the sheath is solidly grounded only at the transformer side (Fig. 11), the results in Fig. 14 show that after applying all the SPDs (including the cable's SVL at the source side, and transformer SAs at HV and LV sides), the peak OVs are almost as high as in the base case where the sheaths are solidly grounded at both sides, and no SPDs are applied.

5. Experimental analysis

An experimental setup, as shown in Fig. 15, has been designed to analyze the effect of the cable sheath grounding configuration on the cable-transformer resonances. The setup consists of a cast-resin dry-type transformer with foil-type windings connected to a cable at the HV terminal. The test cable is an MV-level cable with oil-impregnated paper insulation. It has a length of 27 m and is wound on a spool due to space limitations. The test transformer is connected in a Yy configuration and has a voltage ratio of 21.65/0.525 kV with a nominal capacity of 660 kVA. Because the test cable is single-phase, only one transformer phase is connected to the cable, and the other two phases are disconnected. A Bode-100 model vector network analyzer (VNA), manufactured by Omicron, is applied to measure the
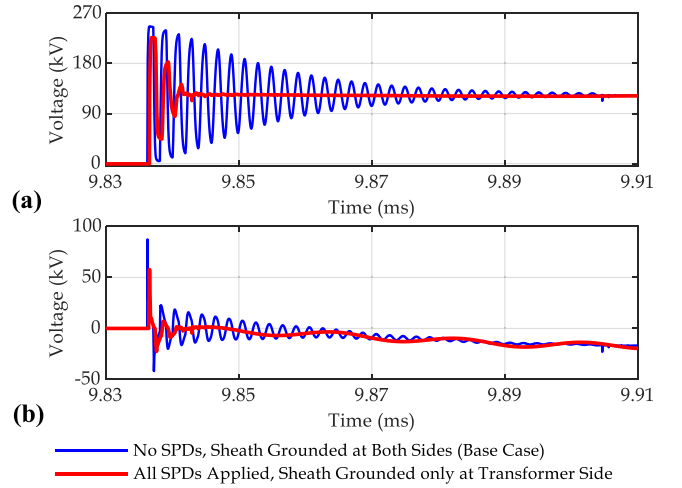

(a)

(b)

Fig. 14. Effect of SVL on cable-transformer system energization transients under single-point sheath grounding configuration at transformer side: (a) Voltage at transformer's HV side, (b) Voltage at transformer's LV side.
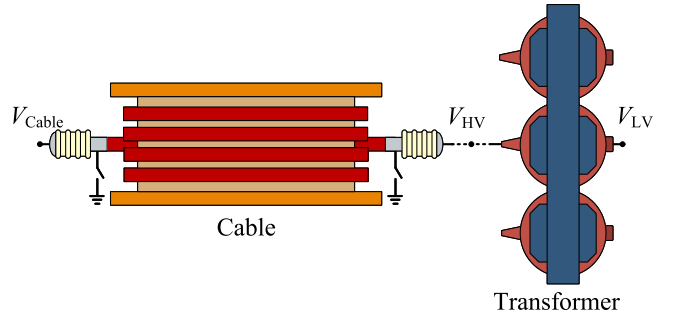

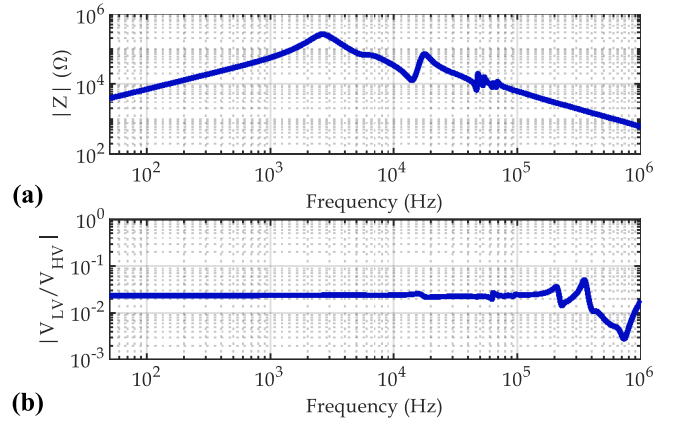Fig. 15. Experimental test setup above view.

(a)

(b)

Fig. 16. Measured frequency response of the test transformer: (a) HV-side terminal impedance, (b) HV to LV transformer ratio.

harmonic impedance and voltage amplification characteristics for a broad frequency range.

Firstly, the test transformer is analyzed without the cable. The harmonic terminal impedance of the HV winding and transformer ratio are shown in Fig. 16.

Next, the cable is connected to the transformer, and the frequency responses of the total test system are measured. The end(s) at which the cable's metallic sheath is grounded can be controlled as shown in Fig. 15. The mutual cable-transformer resonances in the test system
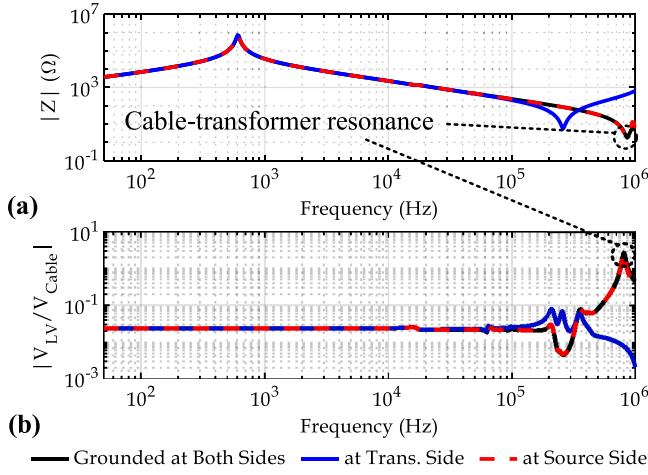
Fig. 17. Measured frequency responses of the test cable-transformer setup: (a) harmonic impedance, (b) transformer ratio.

and the effect of the cable sheath grounding configuration on their formation can be seen in Fig. 17. The experimental results in Fig. 17 confirm that while mutual cable-transformer resonances cause elevated voltage amplifications when the sheath conductor is solidly grounded at both ends or only at the source side, these resonating overvoltages are suppressed when the sheath conductor is grounded only at the transformer side.

6. Conclusions

Mutual interactions between cables and transformers can lead to resonances, which can cause severe OVs and possible insulation damage. The characteristics and terminations of the cable conductors can play an important role in cable-transformer resonances. Here, it is shown that in a cable-transformer system, the different configurations of grounding the metallic sheath of supplying cable can significantly affect the OVs prevailed on transformer terminals.

It is proven that cable quarter-wavelength resonances occur when the metallic sheath is solidly grounded at both sides and when it is only grounded at the source side. In contrast, these resonances are suppressed when single-point grounding is applied at the transformer side.

Subsequently, several analyses are performed on a detailed test system implemented in EMTP. Analyzed frequency responses in EMTP confirm that mutual cable-transformer resonances are suppressed only for the single-point sheath grounding at the transformer side, while they are still present for other sheath grounding configurations.

Furthermore, some case studies are investigated through time-domain simulations in EMTP. The results of energization prestriking analysis show severe resonating OVs occurrence when the sheath is solidly grounded at both ends or only at the source side. However, mutual cable-transformer resonances are not excited when single-point sheath grounding is applied at the transformer side.

Since excessive OVs can affect the OC end of the sheath conductor, an SVL is applied to provide OV protection for the sheath conductor. As a result, it is observed that during the first OV spikes, when the SVL is activated, the cable behaves as if the sheath is solidly grounded at both ends. However, immediately after the SVL is deactivated, mutual cable-transformer resonances are suppressed. In this analysis, the OVs that emerged were below the protection threshold of the SAs at the transformer's terminals. However, it is important to note that the SAs are only effective if the impedance of the ground at the cable-transformer resonance frequency is not significant. Therefore, when

conducting a detailed insulation-coordination analysis, it is essential to implement an accurate wideband model of the ground.

Finally, a laboratory test setup is applied to experimentally validate the effect of cable sheath grounding configuration on cable-transformer resonances. Once again, it is confirmed that mutual cable-transformer resonances and their resultant OV amplifications are suppressed when the sheath conductor is only grounded at the transformer side.

The results from this investigation can be used to mitigate mutual cable-transformer resonances and their resultant OVs. Moreover, by better understanding the mutual impacts between the system components, this research paves the way to develop OV protection schemes against HF transient resonances, especially in modern electrical power systems where such mutual interactions are likely to occur. While this study analyzes the resonances between the supplying cable and the transformer by considering no secondary-side terminations, future research could focus on the mutual resonances between the transformer and cables at its secondary side, analyzing the impact of secondary cable sheath terminations on these resonances.

CRediT authorship contribution statement

Behzad Behdani: Conceptualization, Investigation, Methodology, Formal analysis, Validation, Writing – original draft, Data curation, Visualization, Software, Writing – review & editing. **Mohamad Ghaffarian Niasar:** Investigation, Formal Analysis, Writing – review & editing, Resources, Project administration, Supervision. **Marjan Popov:** Investigation, Project administration, Formal Analysis, Conceptualization, Resources, Writing – review & editing, Funding acquisition, Supervision.

Declaration of competing interest

The authors declare that they have no known competing financial interests or personal relationships that could have appeared to influence the work reported in this paper.

Appendix

Considering Eq. (1), the elements of sub-matrices $\mathbf{Y}_e$ and $\mathbf{Y}_m$ can be obtained with the help of a proper transformation matrix $\mathbf{T}$ by:

$$\mathbf{Y}_e = \begin{bmatrix} A_{11} & A_{12} \\ A_{21} & A_{22} \end{bmatrix}$$
$$= \mathbf{Y}_c \times \left(\mathbf{T} \begin{bmatrix} \coth(\gamma_{m1}l) & 0 \\ 0 & \coth(\gamma_{m2}l) \end{bmatrix} \mathbf{T}^{-1} \right) \tag{A.1}$$

$$\mathbf{Y}_m = \begin{bmatrix} B_{11} & B_{12} \\ B_{21} & B_{22} \end{bmatrix}$$
$$= -\mathbf{Y}_c \times \left(\mathbf{T} \begin{bmatrix} \operatorname{csch}(\gamma_{m1}l) & 0 \\ 0 & \operatorname{csch}(\gamma_{m2}l) \end{bmatrix} \mathbf{T}^{-1} \right) \tag{A.2}$$

where γ_{m1} and γ_{m2} are the modal propagation functions. Through mathematical manipulations, the elements of $\mathbf{Y}_e$ and $\mathbf{Y}_m$ can be expressed as:

$$\mathbf{Y}_e = \begin{bmatrix} a_{11}\coth(\gamma l) & a_{12}\coth(\gamma l) \\ a_{21}\coth(\gamma l) & a_{22}\coth(\gamma l) \end{bmatrix} \tag{A.3}$$

$$\mathbf{Y}_m = \begin{bmatrix} -b_{11}\operatorname{csch}(\gamma l) & -b_{12}\operatorname{csch}(\gamma l) \\ -b_{21}\operatorname{csch}(\gamma l) & -b_{22}\operatorname{csch}(\gamma l) \end{bmatrix} \tag{A.4}$$

where the phase-domain propagation function γ can be characterized in terms of modal propagation functions by:

$$\gamma = \frac{1}{l}\sinh^{-1}\left(\sinh(\gamma_{m1}l) \cdot \sinh(\gamma_{m2}l)\right) \tag{A.5}$$

Data availability

Data will be made available on request.

References

[1] S. Ghasemi, M. Allahbakhshi, B. Behdani, M. Tajdinian, M. Popov, Probabilistic analysis of switching transients due to vacuum circuit breaker operation on wind turbine step-up transformers, Electr. Power Syst. Res. 182 (106204) (2020) 106204, http://dx.doi.org/10.1016/j.epsr.2020.106204.

[2] F. Nasirpour, A. Heidary, M.G. Niasar, A. Lekić, M. Popov, High-frequency transformer winding model with adequate protection, Electr. Power Syst. Res. 223 (109637) (2023) 109637.

[3] CIGRE WG C4.307, Resonance and Ferroresonance in Power Networks, Technical Report TB 569, CIGRE, Paris, France, 2014.

[4] A. Heidary, M.G. Niasar, M. Popov, A. Lekić, Transformer resonance: Reasons, modeling approaches, solutions, IEEE Access 11 (2023) 58692–58704.

[5] G.C. Paap, A. Alkema, L. Van der Sluis, Overvoltages in power transformers caused by no-load switching, IEEE Trans. Power Deliv. 10 (1) (1995) 301–307.

[6] M. Popov, R.P.P. Smeets, L. van der Sluis, H. de Herdt, J. Declercq, Experimental and theoretical analysis of vacuum circuit breaker prestrike effect on a transformer, IEEE Trans. Power Deliv. 24 (3) (2009) 1266–1274.

[7] A. Holdyk, B. Gustavsen, External and internal overvoltages in a 100 MVA transformer during high-frequency transients, in: Proceedings of the IPST Conference, Cavtat, Croatia, 2015, pp. 15–18.

[8] B. Gustavsen, Study of transformer resonant overvoltages caused by cable-transformer high-frequency interaction, IEEE Trans. Power Deliv. 25 (2) (2010) 770–779.

[9] B. Behdani, M. Ghaffarian, M. Popov, Analysis of cable-transformer resonant interactions due to CB prestriking transients, in: 2024 IEEE International Conference on Environment and Electrical Engineering and 2024 IEEE Industrial and Commercial Power Systems Europe (EEEIC/I & CPS Europe), Rome, Italy, 2024, pp. 1–6, http://dx.doi.org/10.1109/EEEIC/ICPSEurope61470.2024.10751644.

[10] P. Akiki, A. Xémard, C. Trouilloud, J.-L. Chanelière, Study of high frequency transient overvoltage caused by cable-transformer quarter-wave resonance, Electr. Power Syst. Res. 197 (2021) 107295.

[11] A. Ametani, T. Ohno, N. Nagaoka, Cable System Transients: Theory Modeling and Simulation, John Wiley & Sons, Nashville, TN, 2015.

[12] Q. Li, et al., Protection performance assessments of two types of sheath voltage limiters in 220kV single point bonded cable system, Electr. Power Syst. Res. 212 (108637) (2022) 108637.

[13] I. Lafaia, et al., Propagation of intersheath modes on underground cables, Electr. Power Syst. Res. 138 (2016) 113–119.

[14] I. Lafaia, et al., Frequency and time domain responses of cross-bonded cables, IEEE Trans. Power Deliv. 33 (2) (2018) 640–648.

[15] H. Xue, J. Mahseredjian, J. Morales, I. Kocar, Analysis of cross-bonded cables using accurate model parameters, IEEE Trans. Power Deliv. 38 (1) (2023) 46–55.

[16] A. Ametani, N. Nagaoka, Yoshihiro, T. Ohno, K. Yamabuki, Power System Transients: Theory and Applications, second ed., CRC Press, London, England, 2020.

[17] V. Brandwajn, H.W. Donnel, I.I. Dommel, Matrix representation of three-phase N-winding transformers for steady-state and transient studies, IEEE Trans. Power Appl. Syst. PAS-101 (6) (1982) 1369–1378.

[18] A. Morched, B. Gustavsen, M. Tartibi, A universal model for accurate calculation of electromagnetic transients on overhead lines and underground cables, IEEE Trans. Power Deliv. 14 (3) (1999) 1032–1038.

[19] TRAGSYS-Software for High Frequency and Transient Analysis of Grounding Systems. [Online]. Available: http://www.tragsys.com/.

[20] L.D. Grcev, Computer analysis of transient voltages in large grounding systems, IEEE Trans. Power Deliv. 11 (2) (1996) 815–823.

[21] J. Gholinezhad, R. Shariatinasab, Interfacing electromagnetic model of tower-footing impedance with the EMTP software package, Int. J. Electr. Power Energy Syst. 105 (2019) 394–403.

[22] M. Popov, L. Grcev, H.K. Hoidalen, B. Gustavsen, V. Terzija, Investigation of the overvoltage and fast transient phenomena on transformer terminals by taking into account the grounding effects, IEEE Trans. Ind. Appl. 51 (6) (2015) 5218–5227.

[23] Modeling of metal oxide surge arresters, IEEE Trans. Power Deliv. 7 (1) (1992) 302–309, http://dx.doi.org/10.1109/61.108922.